Crystal Structure and Magnetic Ordering Transitions in $CeNiIn_4$, $EuNiIn_4$ and $EuCuIn_4$

Walter Schnelle[a], Reinhard K. Kremer[b], Rolf-Dieter Hoffmann[c], Ute Ch. Rodewald[c], and Rainer Pöttgen[c]

[a] Max-Planck-Institut für Chemische Physik fester Stoffe, Nöthnitzer Straße 40, 01187 Dresden, Germany
[b] Max-Planck-Institut für Festkörperforschung, Heisenbergstraße 1, 70569 Stuttgart, Germany
[c] Institut für Anorganische und Analytische Chemie, Universität Münster, Corrensstraße 30, 48149 Münster, Germany

Reprint requests to R. Pöttgen. E-mail: pottgen@uni-muenster.de

Z. Naturforsch. **2014**, *69b*, 1003 – 1009 / DOI: 10.5560/ZNB.2014-4192
Received August 24, 2014

Polycrystalline $CeNiIn_4$ was prepared by arc-melting of the elements and subsequent annealing at 970 K in vacuum. $EuNiIn_4$ and $EuCuIn_4$ were synthesized from the elements by reactions in sealed tantalum tubes. These indium-rich compounds crystallize with the $YNiAl_4$-type structure which was refined for $EuCuIn_4$ from single-crystal X-ray diffraction data: *Cmcm*, $a = 450.04(9)$, $b = 1698.7(4)$, $c = 740.2(2)$ pm, $wR2 = 0.0606$, 495 F^2 values, 24 variables. The $EuCuIn_4$ structure is built up from a complex three-dimensional $[CuIn_4]$ polyanion (265 – 279 pm Cu–In and 296 – 331 pm In–In) in which the europium atoms occupy distorted hexagonal channels. The Eu–Eu distances within these channels (450 pm) are significantly shorter than the distances between Eu atoms in neighboring channels (552 pm). The magnetic properties and the specific heats of the europium compounds have been investigated. Both europium compounds show the magnetism of divalent Eu ions and antiferromagnetic ordering at low temperatures. $EuCuIn_4$ is magnetically ordered *via* a surprisingly complex sequence of three transitions.

Key words: Indide, Europium Compounds, $YNiAl_4$ Type, Magnetic Properties, Resistivity, Specific Heat

Introduction

The $YNiAl_4$ structure [1] is one of the important structure types for triel-rich intermetallic compounds. The Pearson data base [2] lists more than 40 representatives in the field of aluminides, gallides and indides. From a geometrical point of view one can derive the $YNiAl_4$ type through an insertion of additional aluminum layers into the Re_3B-type $YNiAl_2$. This crystal-chemical peculiarity has been discussed in detail [1, 3, 4].

Most crystal structure work on these so-called 1-1-4 phases has been performed for the indides. The largest series of compounds is formed with the rare-earth elements and nickel: *RE*$NiIn_4$ for *RE* = La–Nd, Eu and Yb [3, 5 – 9]. Isoelectronic compounds can be synthesized with palladium and platinum: *RE*$PdIn_4$ with *RE* = Ce, Eu and Yb [10, 11] and *RE*$PtIn_4$ with *RE* = La, Eu and Yb [4, 12 – 14]. Variation of the valence electron count is possible by using a more electron-rich transition metal or *via* substitution of the trivalent rare earth elements by alkaline earth metals, leading to the indides $CaNiIn_4$ [15], $CaPdIn_4$ [16], Sr*T*In_4 (*T* = Ni, Pd, Pt) [17], $EuCuIn_4$ [15, 18], and $EuAuIn_4$ [19].

So far only a few of the $YNiAl_4$-type compounds have been studied with respect to their physical properties: $EuNiIn_4$ [3] was found to be an antiferromagnet below 16 K, and $CeNiAl_4/CeNiIn_4$-based solid solutions were tested for application as thermoelectric materials [7]. An intermediate valence has been observed for europium by X-ray absorption L_{III} spectroscopy [18].

Complex double magnetic phase transitions have been detected in $CeNiIn_4$ and $EuPtIn_4$ single crystals [9, 13, 14]. $TbNiAl_4$ also exhibits two magnetic phase transitions at 34 and 28 K [20]. Powder neutron

diffraction data showed an incommensurate magnetic ordering between 34 and 28 K and a collinear antiferromagnetic structure as the low-temperature ground state.

In the course of our systematic studies on structure-property relationships of binary and ternary intermetallic indium compounds [3, 6, 10, 21 – 23] we mainly focused on cerium- and europium-containing members with a special attention on potential valence changes. In this contribution we report on the crystal structure, and the magnetic and thermal properties of polycrystalline $CeNiIn_4$, $EuNiIn_4$ and $EuCuIn_4$ phases. Magnetic susceptibility and specific heat data manifest magnetic ordering at low temperature. The high-temperature magnetic susceptibility data confirm the predominantly divalent valence of europium in $EuNiIn_4$ and $EuCuIn_4$. The structure of $EuCuIn_4$ was refined from single-crystal X-ray diffraction data.

Experimental

Synthesis

Starting materials for the preparation of the polycrystalline $CeNiIn_4$, $EuNiIn_4$ and $EuCuIn_4$ samples were ingots of cerium and europium (Johnson Matthey), nickel wire (Johnson Matthey, ∅ 0.18 mm), copper wire (Johnson Matthey, ∅ 0.38 mm), and indium tear drops (Johnson Matthey), all with stated purities better than 99.9 %. The larger ingots of cerium and europium were mechanically cut into small pieces in an argon-filled glove box and subsequently stored in Schlenk tubes prior to the synthesis. The argon was purified over titanium sponge (900 K) and molecular sieves.

In a first step, cerium buttons were fused by arc-melting small irregular cerium pieces in a miniaturized arc-melting furnace [24]. In a second step, the cerium buttons, nickel wire, and indium tear drops in 1 : 1 : 4 atomic ratios were arc-melted together. The buttons were re-melted several times to ensure homogeneity. The total weight loss after completion of the melting procedures was less than 0.5 weight-%. The sample buttons were subsequently sealed in evacuated silica ampoules and annealed at 970 K for two weeks in a tube furnace.

Due to the high vapor pressure of europium, a simple synthesis *via* arc-melting is not possible for $EuNiIn_4$ and $EuCuIn_4$. Here, the elemental components were mixed in the ideal atomic ratios and sealed in tantalum tubes under an argon pressure of about 800 mbar. The tantalum tubes were annealed in an argon-flushed water-cooled sample chamber in a high-frequency furnace (Kontron, type Roto-Melt, 1.2 kW) [25]. In a first step the tubes were heated with the maximum powder output of the high-frequency generator. The strongly exothermic reactions are easily visibly by a heat flash for about one second. The annealing temperature was then lowered to about 1000 K for about one minute and then raised again to the maximum. Subsequently the tubes were annealed for two hours at about 800 K. The reactions resulted in light-gray polycrystalline samples of $EuNiIn_4$ and $EuCuIn_4$ which could easily be separated from the tantalum tube without any tantalum contamination (checked by EDX analyses). Powders of both compounds are stable in air. No decomposition was observed after several months

X-Ray diffraction

The powdered polycrystalline $EuCuIn_4$ sample was characterized by Guinier X-ray diffraction patterns (classical film data) using CuK_{α_1} radiation and α-quartz ($a = 491.30$, $c = 540.46$ pm) as an internal standard. The orthorhombic lattice parameters (Table 1) were obtained from a least-squares refinement. Correct indexing of the pattern was ensured by an intensity calculation [26]. The present data show good agreement with those determined by Sysa and Kalychak ($a = 449.3(2)$, $b = 1693.5(5)$, $c = 737.3(5)$ pm) [15]. The patterns of $CeNiIn_4$ and $EuNiIn_4$ were in agreement with previous literature data [3, 6], indicating phase-pure samples for property studies.

Table 1. Crystal data and structure refinement for $EuCuIn_4$.

Empirical formula	$EuCuIn_4$
Molar mass, g mol^{-1}	674.78
Lattice parameters (Guinier data)	
a, pm	450.04(9)
b, pm	1698.7(4)
c, pm	740.2(2)
Cell volume V, nm^3	0.5659
Space group, Z	*Cmcm*, 4
Pearson symbol	*oC*24
Calculated density, g cm^{-3}	7.92
Crystal size, μm^3	30 × 30 × 30
Transmission ratio (max/min)	1.04
Absorption coefficient, mm^{-1}	30.5
F(000), e	1152
θ range, deg	2 – 30
Range in *hkl*	+6, ±23, ±10
Total no. of reflections	1815
Independent reflections, R_{int}	495/0.0490
Reflections with $I > 2\,\sigma(I)$, R_{sigma}	375/0.0369
Data/parameters	495/24
Goodness-of-fit on F^2	1.079
$R1/wR2$ for $I > 2\,\sigma(I)$	0.0256/0.0532
$R1/wR2$ for all data	0.0457/0.0606
Extinction coefficient	0.00063(8)
Largest diff. peak and hole, e Å^{-3}	2.41/−1.99

Table 2. Atomic coordinates and displacement parameters (pm^2) for $EuCuIn_4$. U_{eq} is defined as one third of the trace of the orthogonalized U_{ij} tensor. Coefficients U_{ij} of the anisotropic displacement factor tensor of the atoms are defined by: $-2\pi^2[(ha^*)^2U_{11}+...+2hka^*b^*U_{12}]$. $U_{12}=U_{13}=0$.

Atom	Wyckoff site	x	y	z	U_{11}	U_{22}	U_{33}	U_{23}	U_{eq}
Eu	4*c*	0	0.12062(4)	1/4	86(4)	106(4)	141(4)	0	111(2)
Cu	4*c*	0	0.77208(12)	1/4	93(9)	141(9)	136(9)	0	123(4)
In1	8*f*	0	0.31471(4)	0.05016(10)	94(4)	133(4)	92(3)	−4(3)	106(2)
In2	4*c*	0	0.92783(7)	1/4	134(6)	110(5)	192(5)	0	145(3)
In3	4*b*	0	1/2	0	125(6)	132(5)	224(6)	−11(4)	160(3)

Irregularly shaped crystals of $EuCuIn_4$ were selected from the annealed sample by careful mechanical fragmentation. They were glued to quartz fibers using beeswax and investigated by Laue photographs on a Buerger camera (white molybdenum radiation, image plate technique, Fujifilm, BAS-1800) in order to check crystal quality and suitability for intensity data collection. Single-crystal diffraction intensities were collected at room temperature on a four-circle diffractometer (CAD4) with graphite-monochromatized MoK_α radiation ($\lambda = 0.71073$ pm) and a scintillation counter with pulse height discrimination. The scans were performed in the $\omega/2\theta$ mode. An empirical absorption correction was applied on the basis of ψ-scan data. Details of the data collection and the structure refinement are listed in Table 1.

Structure refinement

Analyses of the $EuCuIn_4$ intensity data set revealed a *C*-centered orthorhombic lattice. The systematic extinctions were in accordance with space group *Cmcm*, in agreement with earlier studies on $EuNiIn_4$ [3] and $EuPdIn_4$ [10]. Since isotypism with the latter indides ($YNiAl_4$ type [1]) was already evident from the Guinier powder pattern, the atomic parameters of $EuPdIn_4$ [10] were taken as starting values, and the structure was refined on F^2 with anisotropic displacement parameters for all atoms employing the SHELXL-97 software package [27] (full-matrix least-squares refinement on F^2). Variation of the occupancy parameters in a separate series of least-squares refinements gave no indication for deviations from the ideal composition. The final difference Fourier synthesis revealed no significant residual electron density peaks. The refined positional parameters and interatomic distances are listed in Tables 2 and 3.

Further details of the crystal structure investigation may be obtained from Fachinformationszentrum Karlsruhe, 76344 Eggenstein-Leopoldshafen, Germany (fax: +49-7247-808-666; e-mail: crysdata@fiz-karlsruhe.de, http://www.fiz-karlsruhe.de/request_for_deposited_data.html) on quoting the deposition number CSD-427818.

Table 3. Interatomic distances (pm), calculated with the lattice parameters taken from powder X-ray diffraction data of $EuCuIn_4$. All distances within the first coordination spheres are listed. Standard deviations are equal or less than 0.2 pm.

Eu:	1	In2	327.5	In1:	1	Cu	266.6
	4	In1	334.8		2	Cu	278.9
	2	Cu	341.8		1	In1	295.9
	4	In3	356.2		1	In3	316.9
	2	In1	361.4		2	In1	323.2
	2	In2	379.1		2	In2	330.8
	2	Cu	412.6		2	Eu	334.8
	2	Eu	450.0		1	Eu	361.4
Cu:	1	In2	264.6	In2:	1	Cu	264.6
	2	In1	266.6		4	In3	316.1
	4	In1	278.9		1	Eu	327.5
	2	Eu	341.8		4	In1	330.8
	2	Eu	412.6		2	Eu	379.1
				In3:	4	In2	316.1
					2	In1	316.9
					4	Eu	356.2

Physical property measurements

The magnetization was measured in a commercial SQUID magnetometer (MPMS, Quantum Design). The specific heat $C_P(T)$ was determined by a quasi-adiabatic heat pulse method on home-built Nernst-type calorimeters with sapphire sample holders. Measurements were made between 1.5 and 60 K; for $CeNiIn_4$ a ^{3}He cryostat was employed from 0.58 to 1.54 K. For each compound the lattice contribution $C_{lat}(T)$ was estimated based on a conversion of $C_P(T)$ to equivalent Debye temperature. Magnetic contributions to the specific heat are calculated as $C_{mag} = C_P - C_{lat}$.

Discussion

Crystal chemistry

The structure of $EuCuIn_4$ was previously characterized only on the basis of powder X-ray diffraction data [15]. The present single-crystal investiga-

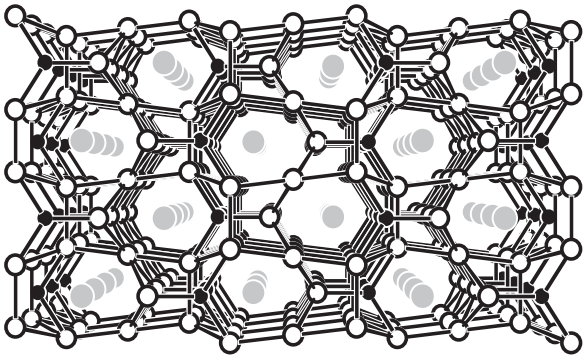

Fig. 1. Perspective view of the $EuCuIn_4$ structure along the crystallographic *a* axis. The europium, copper and indium atoms are drawn as gray, small black and open circles, respectively. The three-dimensional $[CuIn_4]$ polyanion is emphasized.

tion essentially confirms the previous refinement; however, the atom positions were determined more accurately, especially for the more weakely (with respect to europium and indium) scattering copper atoms. The largest difference between both structure refinements therefore occurs for the *y* parameter of copper: 0.763(3) as determined from powder data and 0.77208(12) for the present refinement.

Since the crystal chemistry of the $YNiAl_4$-type indium compounds has been discussed in detail in references [3, 6, 16] for isotypic $CeNiIn_4$, $EuNiIn_4$ and $CaPdIn_4$, herein we give only a brief illustration for $EuCuIn_4$. As outlined in Fig. 1, the $EuCuIn_4$ structure is composed of a three-dimensional $[CuIn_4]$ polyanion in which the europium atoms are embedded in distorted hexagonal channels. Within these channels we observe Eu–Eu distances of 450 pm. These correspond to the lattice parameter *a*. Eu–Eu distances between Eu atoms in adjacent channels are larger than 552 pm.

The shortest interatomic distances in the $[CuIn_4]$ polyanion occur between the copper and indium atoms. Each copper atom has three short Cu–In contacts: 1×265 and 2×267 pm. These distances compare well with the sum of Pauling's single bond radii [28] of 267 pm for copper and indium, indicating strong covalent Cu–In bonding. In addition each copper atom has four slightly longer Cu–In contacts at 279 pm.

Comparing Pearson's absolute electronegativities of 4.48 eV for copper and 3.10 eV for indium [28], it is evident that the europium atoms are the most electropositive constituents of $EuCuIn_4$. In a first approximation the Eu atoms will transfer their two valence electrons (consistent with the magnetic susceptibility data) to the more electronegative copper and indium atoms. Considering the essentially covalent Cu–In and In–In bonding within the three-dimensional polyanion, the chemical formula can be written as $Eu^{2+}[CuIn_4]^{2-}$.

The three crystallographically different indium atoms show a variety of In–In contacts which cover the large range from 296 to 331 pm. Each indium atom has at least four short In–In contacts. These In–In distances are shorter than the In–In distances in the tetragonal body-centered structure of elemental indium ($a = 325.2$, $c = 494.7$ pm [29]), where each indium atom has four nearest neighbors at 325 pm and eight further neighbors at 338 pm with an average In–In distance of 334 pm. The In1 atoms have only six indium neighbors, while In2 and In3 have eight near indium neighbors which form strongly distorted cubes. Thus, the $EuCuIn_4$ structure contains different distortions of approximately tetragonal body-centered indium fragments. Such indium units are frequently observed in indium-rich intermetallic compounds as discussed in more detail in references [10, 16].

Physical properties

In agreement with previous determinations [9], the magnetic susceptibility of $CeNiIn_4$ follows a Curie-Weiss law at high temperatures (range of fit 60 – 300 K). The effective paramagnetic moment μ_{eff} of 2.4 μ_B indicates stable-valent Ce^{3+} with the $^2F_{5/2}$ ground state of the $4f^1$ configuration. The Weiss temperature is small ($\theta = -2$ K). Magnetic specific heat data (Fig. 2) reveal a mean-field type anomaly at $T_{N1} = 1.40(3)$ K indicating long-range magnetic ordering of the Ce moments. A very sharp lambda peak at $T_{N2} = 0.74(2)$ K signals a change of the spin structure. The magnetic entropy $S_{mag}(T)$ above T_{N1} is close to R ln2 (R = molar gas constant), indicating a doublet ground state and a negligible influence of the Kondo effect. The increase of c_{mag}/T above 5.5 K is due to crystal field excitations. All these findings are in good agreement with those in a previous comprehensive investigation by Shishido *et al.* [9].

The magnetic susceptibility $\chi(T)$ of both Eu compounds (Fig. 3) is well described by the Curie-Weiss law at high temperatures (range of fit 80 – 300 K). The resulting μ_{eff} and θ values are 7.66 μ_B and -14.0 K for $EuNiIn_4$ and 7.13 μ_B and –7.2 K for $EuCuIn_4$.

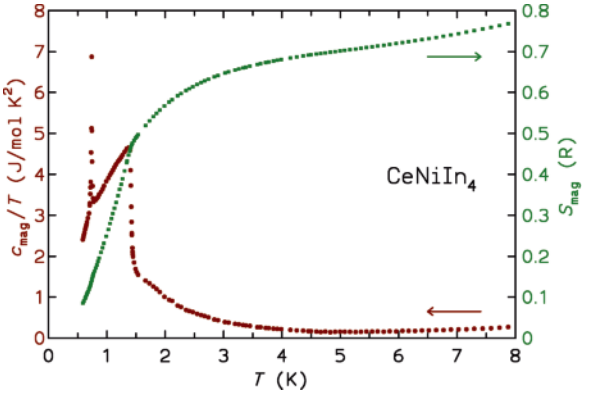

Fig. 2 (color online). Magnetic contribution to the specific heat of $CeNiIn_4$ in a $c_{\rm mag}(T)/T$ representation and magnetic entropy $S_{\rm mag}(T)$.

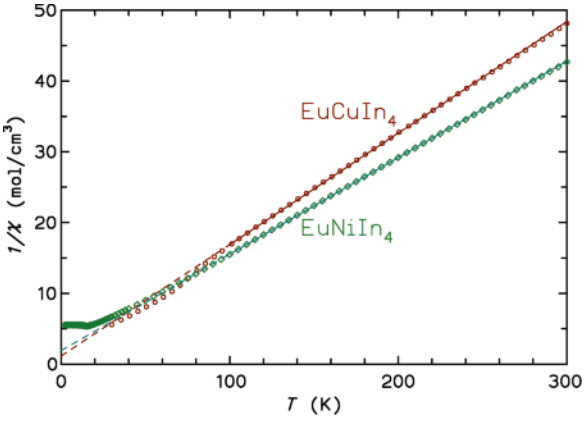

Fig. 3 (color online). Inverse magnetic susceptibilities (cgs), $1/\chi(T)$, of $EuNiIn_4$ and $EuCuIn_4$. The Curie-Weiss fits (see text) are indicated by continuous lines, the extrapolations to zero temperature by dashed lines.

Whereas $\mu_{\rm eff}$ of $EuNiIn_4$ is in the range consistent with stable-valent Eu^{2+} compounds ($^8S_{7/2}$ ground state of the $4f^7$ configuration), for $EuCuIn_4$ an admixture of the $4f^6$ configuration (Eu^{3+}) cannot be excluded. The antiferromagnetic ordering of the Eu moments in $EuNiIn_4$ is clearly visible from a cusp in $\chi(T)$ at $T_{\rm N} = 15.5(5)$ K. For $EuCuIn_4$ the situation appears to be more complicated (details not shown here): immediately visible is a sudden increase of $\chi(T)$ in small applied fields at $T_{\rm fm} = 5.5$ K which points to an ordered phase with a small ferromagnetic moment. Below $T_{\rm afm} = 2.7$ K, $\chi(T)$ decreases sharply indicating a purely antiferromagnetic phase. Interestingly, there exist also small cusp-like anomalies in the temperature

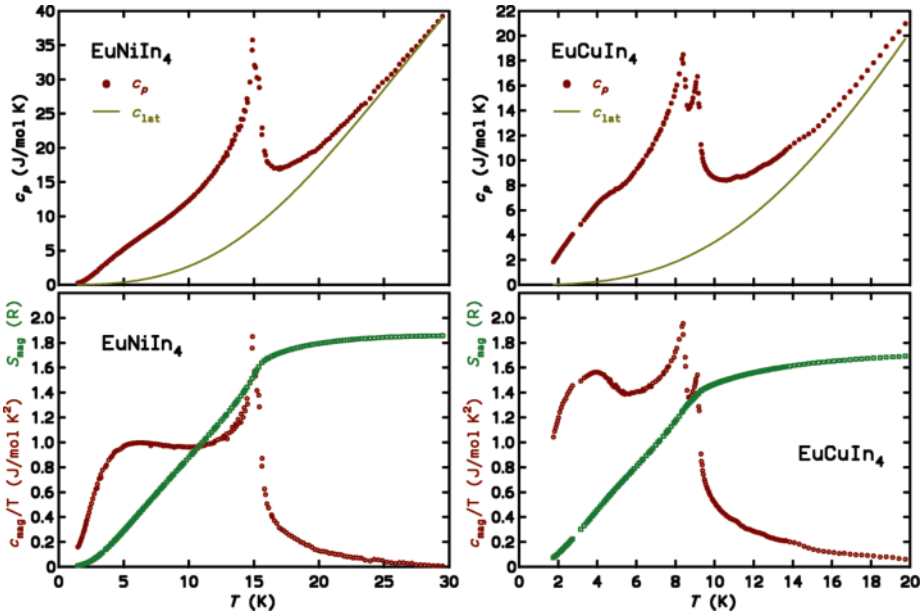

Fig. 4 (color online). Specific heat $C_{\rm P}(T)$ of $EuNiIn_4$ (left) and $EuCuIn_4$ (right). The estimated lattice contributions $C_{\rm lat}(T)$ are indicated as full lines. The lower panels show the magnetic contributions divided by temperature, $C_{\rm mag}(T)/T$, as well as the magnetic entropies $S_{\rm mag}(T)$.

range 8.5 – 9.0 K. Specific heat data were subsequently collected in order to shed more light on this rather complicated magnetic behavior.

The specific heat $C_P(T)$ of $EuNiIn_4$ and $EuCuIn_4$ and the entropy analysis are depicted in Fig. 4. For $EuNiIn_4$ the lambda-type anomaly with two closely neighboring peaks at $T_{N1} = 15.3$ K and $T_{N2} = 14.9$ K and with a broad hump around 6 K is in agreement with the magnetic susceptibility data. A broad hump-like anomaly well below T_N is a typical hallmark of the Zeeman splitting of a highly degenerate multiplet (8 singlets for $4f^7$ systems). The magnetic entropy S_{mag}, obtained as the integral over C_{mag}/T well above T_{N1} is around 1.84 R for $EuNiIn_4$, close to the expected value R ln8. Thus, $EuNiIn_4$ shows the typical picture of antiferromagnetic ordering, possibly with an intermediate phase existing only between T_{N1} and T_{N2}.

For the Cu compound a lambda-type anomaly with two clearly separated peaks at $T_{N1} = 9.1$ K and $T_{N2} = 8.4$ K is observed. Interestingly, these clear anomalies correspond to the unobtrusive anomalies in $\chi(T)$ in this temperature range. The hump-like anomaly well below is different from that for the Ni compound: it is sharper, and a closer inspection reveals a kink at ≈ 5.4 K, corresponding to the appearance of the ferromagnetic component at T_{fm} in $\chi(T)$. Thus, the magnetic moments in $EuCuIn_4$ are ordered first in antiferromagnetic structures at T_{N1} and T_{N2}, and are then rearranged at T_{fm} to a structure with a small uncompensated moment, and finally are transformed to a fully antiferromagnetic structure below T_{afm}. As judged from the specific heat and entropy data, these successive transitions originate from the main phase. The integrated magnetic entropy S_{mag} above T_{N1} is around 1.70 R, significantly below the expected value R ln8.

The lower than expected value for S_{mag}, as well as the observation of a reduced μ_{eff}, shed some doubt on the stable divalent nature of europium in $EuCuIn_4$. In a naive estimate, both findings indicate that only 82 % of the Eu species are in the $4f^7$ electronic configuration. An even larger contribution of the f^6 configuration has been concluded by Sysa *et al.* from X-ray absorption data at the L_{III} edge [18]. Further spectroscopic investigations are required to clarify the valence configuration of Eu in $EuCuIn_4$.

Acknowledgement

This work was financially supported by the Deutsche Forschungsgemeinschaft. We thank E. Brücher, K. Ripka and E. Schmitt for assistance during the measurements. Our special thanks go to Dr. R. W. Henn for experimental assistance.

[1] R. M. Rykhal', O. S. Zarechnyuk, Ya. P. Yarmolyuk, *Sov. Phys. Crystallogr.* **1972**, *17*, 453.
[2] P. Villars, K. Cenzual, *Pearson's Crystal Data: Crystal Structure Database for Inorganic Compounds* (release 2013/14), ASM International®, Materials Park, Ohio (USA) **2013**.
[3] R. Pöttgen, R. Müllmann, B. D. Mosel, H. Eckert, *J. Mater. Chem.* **1996**, *6*, 801.
[4] Ya. V. Galadzhun, R. Pöttgen, *Z. Anorg. Allg. Chem.* **1999**, *625*, 481.
[5] Ya. M. Kalychak, V. M. Baranyak, V. I. Zaremba, P. Yu. Zavalii, O. V. Dmytrakh, V. A. Bruskov, *Sov. Phys. Crystallogr.* **1988**, *33*, 602.
[6] R. Pöttgen, *J. Mater. Chem.* **1995**, *5*, 769.
[7] K. M. Poduska, F. J. DiSalvo, V. Petříček, *J. Alloys Compd.* **2000**, *308*, 64.
[8] Ya. M. Kalychak, V. I. Zaremba, Ya. V. Galadzhun, Kh. Yu. Miliyanchuk, R.-D. Hoffmann, R. Pöttgen, *Chem. Eur. J.* **2001**, *7*, 5343.
[9] H. Shishido, N. Nakamura, T. Ueda, R. Asai, A. Galatanu, E. Yamamoto, Y. Haga, T. Takeuchi, Y. Narumi, T. C. Kobayashi, K. Kindo, K. Sugiyama, T. Namiki, Y. Aoki, H. Sato, Y. Ōnuki, *J. Phys. Soc. Jpn.* **2004**, *73*, 664.
[10] R.-D. Hoffmann, R. Pöttgen, V. I. Zaremba, Ya. M. Kalychak, *Z. Naturforsch.* **2000**, *55b*, 834.
[11] S. N. Nesterenko, A. I. Tursina, D. V. Shtepa, H. Noel, Y. D. Seropegin, *J. Alloys Compd.* **2007**, *442*, 93.
[12] V. I. Zaremba, U. Ch. Rodewald, R.-D. Hoffmann, Ya. M. Kalychak, R. Pöttgen, *Z. Anorg. Allg. Chem.* **2003**, *629*, 1157.
[13] P. Kushwaha, A. Thamizhavel, A. K. Nigam, S. Ramakrishnan, *Crystal Growth Design* **2014**, *14*, 2747.
[14] P. F. S. Rosa, C. B. R. de Jesus, Z. Fisk, P. G. Pagliuso, *J. Magn. Magn. Mater.* **2014**, *371*, 5.
[15] L. V. Sysa, Ya. M. Kalychak, *Kristallografiya* **1993**, *38*, 271.
[16] R.-D. Hoffmann, R. Pöttgen, *Chem. Eur. J.* **2000**, *6*, 600.
[17] I. Muts, V. I. Zaremba, V. V. Baran, R. Pöttgen, *Z. Naturforsch.* **2007**, *62b*, 1407.

[18] L. V. Sysa, Ya. M. Kalychak, I. N. Stets', Ya. V. Galadzhun, *Crystallogr. Rep.* **1994**, *39*, 743.
[19] S. Sarkar, M. J. Gutmann, S. C. Peter, *Crystal Growth Design* **2013**, *13*, 4285.
[20] W. D. Hutchinson, D. J. Goossens, K. Nishimura, K. Mori, Y. Isikawa, A. J. Studer, *J. Magn. Magn. Mater.* **2006**, *301*, 352.
[21] R. Pöttgen, *J. Mater. Chem.* **1996**, *6*, 63.
[22] R. Pöttgen, *Z. Kristallogr.* **1996**, *211*, 884.
[23] R. Müllmann, B. D. Mosel, H. Eckert, G. Kotzyba, R. Pöttgen, *J. Solid State Chem.* **1998**, *137*, 174.
[24] R. Pöttgen, T. Gulden, A. Simon, *GIT Labor-Fachzeitschrift* **1999**, *43*, 133.
[25] A. Lang, R.-D. Hoffmann, B. Künnen, G. Kotzyba, R. Müllmann, B. D. Mosel, C. Rosenhahn, *Z. Kristallogr.* **1999**, *214*, 143.
[26] K. Yvon, W. Jeitschko, E. Parthé, *J. Appl. Crystallogr.* **1977**, *10*, 73.
[27] G. M. Sheldrick, *Acta Crystallogr.* **2008**, *A64*, 112.
[28] J. Emsley, *The Elements*, Oxford University Press, Oxford **1999**.
[29] J. Donohue, *The Structures of the Elements*, Wiley, New York **1974**.